Supporting Information

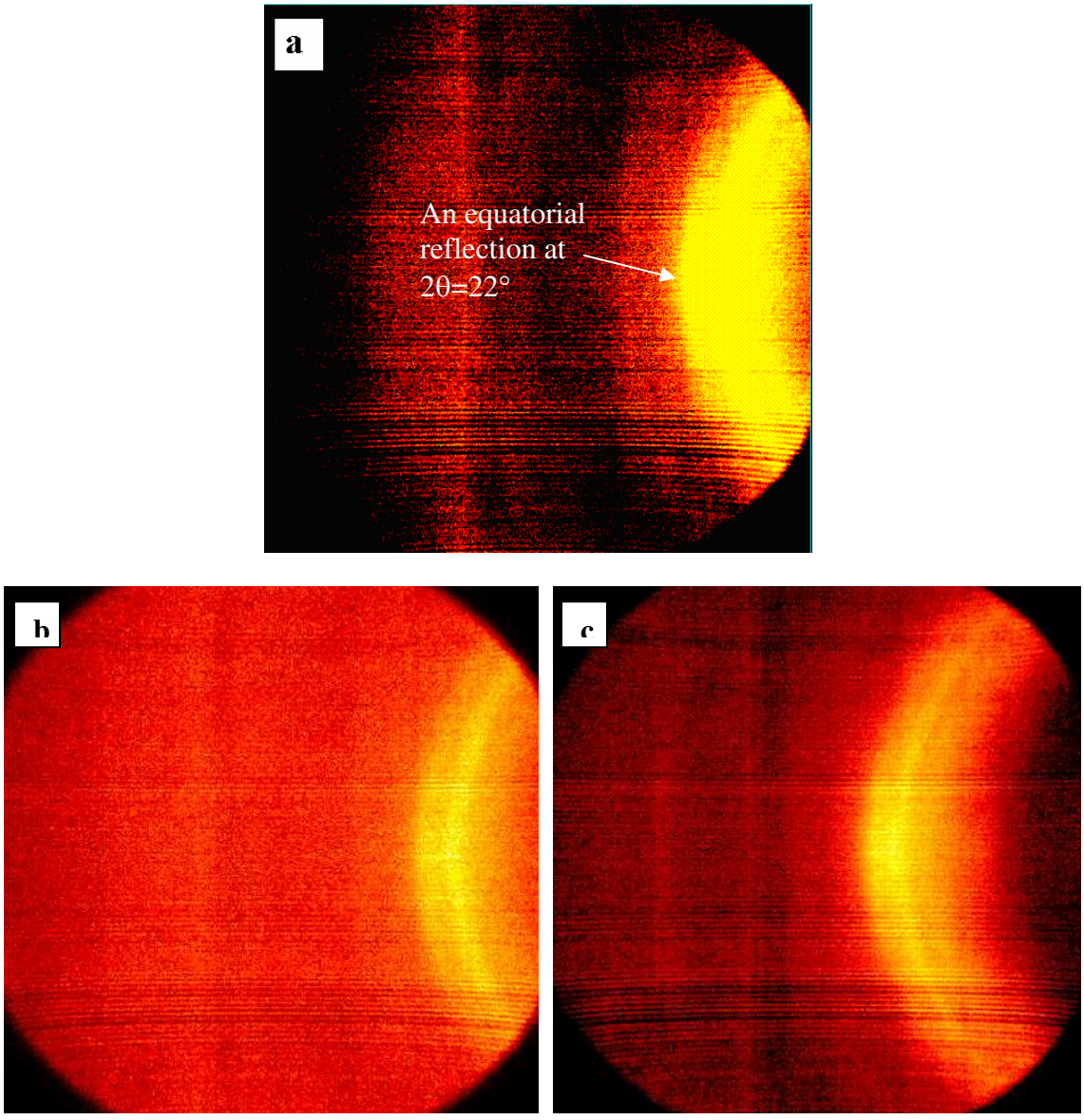

Figure S1 2D WAXD patterns of electrospun fibrous thin films of (a) PVDF, (b) PVDF/MWCNT and (c) PVDF/SWCNT. The CNT concentration is 0.01 wt.% in (b) and (c).

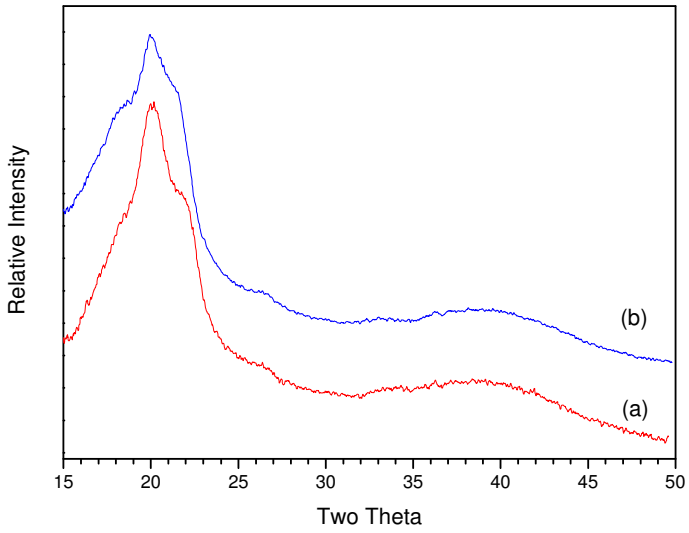

Figure S2. WAXD patterns of the aligned electrospun fibrous thin films of (a) PVDF/MWCNT and (b) PVDF/SWCNT. The CNT concentration is 0.1 wt.%. Compared with the composite nanofibers containing 0.01 wt.% CNT, the shoulder peak at 2θ = 21.5° is weakened for the PVDF/SWCNT but enhanced for the PVDF/MWCNT probably due to the conflicting effects of the higher concentration and poorer dispersion state of the CNTs.

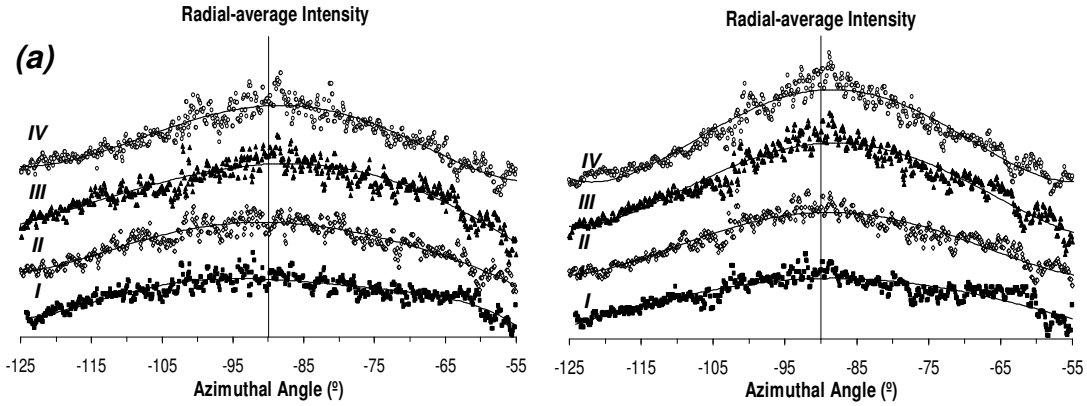

Figure S3. WAXD intensity versus azimuthal angle plots for the equatorial reflections of (a) PVDF/MWCNT and (b) PVDF/SWCNT. The curve I, II, III and IV are radial-average intensity in the 2θ range of 18°-19°, 19°-20°, 20°-21° and 21°-23°, respectively. The solid lines are Lorentzian fitting curves. The CNT concentration is 0.1 wt.%.

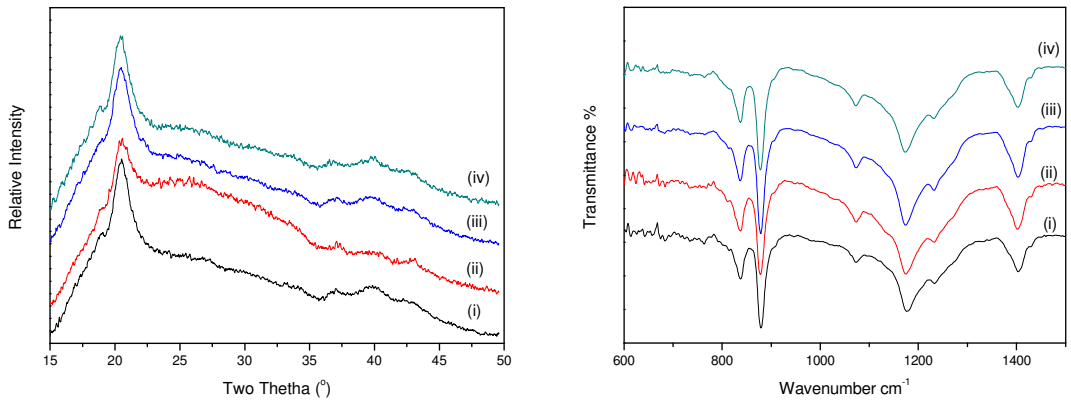

Figure S4 (a) WAXD patterns and (b) FTIR spectra of spin-coated PVDF/MWCNT thin films with CNT concentration of (i) 0.001 wt.%, (ii) 0.01 wt.%, (iii) 0.1 wt.% and (iv) 0.5 wt.%.

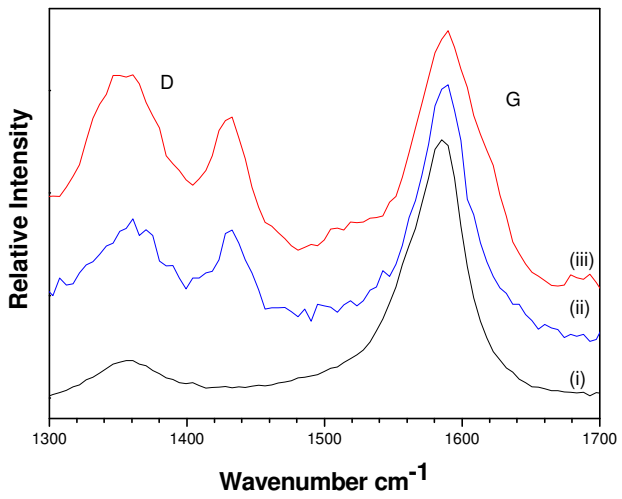

Figure S5 Raman spectra of (i) polystyrene-grafted SWCNT (SWCNT-PS; the content of the grafted PS is about 47 wt.%), (ii) spin-coated PVDF/SWCNT-PS thin film and (iii) electrospun PVDF/SWCNT-PS fibrous thin film showing that the drastic change in the G/D ratio for the electrospun sample is not caused by the sonication process as the spin-coated sample has gone through the same process. The concentration of the SWCNT-PS is 0.1 wt.% in (ii) and (iii).